# Kinetics and Crystal Structure of the Wild-Type and the Engineered Y101F Mutant of *Herpes simplex* Virus Type 1 Thymidine Kinase Interacting with (North)-methanocarba-thymidine[†,‡]

Andrea Prota,[§,||] Joachim Vogt,[||,⊥] Beatrice Pilger,[§,#] Remo Perozzo,[§,▽] Christine Wurth,[§] Victor E. Marquez,[▼] Pamela Russ,[▼] Georg E. Schulz,[⊥] Gerd Folkers,[§] and Leonardo Scapozza*[,§]

*Department of Applied BioSciences, Swiss Federal Institute of Technology (ETH), Winterthurerstrasse 190, CH-8057 Zürich, Switzerland, Institut für Organische Chemie und Biochemie, Albert-Ludwigs-Universität, Albertstrasse 21, D-79104 Freiburg im Breisgau, Germany, and Laboratory of Medicinal Chemistry, Division of Basic Sciences, National Cancer Institute, National Institutes of Health, Bethesda, Maryland 20892*

*Received March 24, 2000; Revised Manuscript Received May 30, 2000*

ABSTRACT: Kinetic and crystallographic analyses of wild-type *Herpes simplex* virus type 1 thymidine kinase ($TK_{HSV1}$) and its Y101F-mutant [$TK_{HSV1}$(Y101F)] acting on the potent antiviral drug 2′-*exo*-methanocarba-thymidine (MCT) have been performed. The kinetic study reveals a 12-fold $K_M$ increase for thymidine processed with Y101F as compared to the wild-type $TK_{HSV1}$. Furthermore, MCT is a substrate for both wild-type and mutant $TK_{HSV1}$. Its binding affinity for $TK_{HSV1}$ and $TK_{HSV1}$(Y101F), expressed as $K_i$, is 11 $\mu$M and 51 $\mu$M, respectively, whereas the $K_i$ for human cytosolic thymidine kinase is as high as 1.6 mM, rendering $TK_{HSV1}$ a selectivity filter for antiviral activity. Moreover, $TK_{HSV1}$(Y101F) shows a decrease in the quotient of the catalytic efficiency ($k_{cat}/K_M$) of dT over MCT corresponding to an increased specificity for MCT when compared to the wild-type enzyme. Crystal structures of wild-type and mutant $TK_{HSV1}$ in complex with MCT have been determined to resolutions of 1.7 and 2.4 Å, respectively. The thymine moiety of MCT binds like the base of dT while the conformationally restricted bicyclo[3.1.0]-hexane, mimicking the sugar moiety, assumes a 2′-*exo* envelope conformation that is flatter than the one observed for the free compound. The hydrogen bond pattern around the sugar-like moiety differs from that of thymidine, revealing the importance of the rigid conformation of MCT with respect to hydrogen bonds. These findings make MCT a lead compound in the design of resistance-repellent drugs for antiviral therapy, and mutant Y101F, in combination with MCT, opens new possibilities for gene therapy.

*Herpes simplex* virus type 1 (HSV1) is a well-characterized widespread infectious agent in human populations (*1*, *2*). HSV1 infections are associated with oral-facial and skin lesions. Especially in immunocompromised hosts, HSV1 infections can cause severe conditions, namely, blindness and central nervous system damage (*3*). During the past decade, potent agents against herpes virus infections have been found. The mode of action of these drugs is based on the different substrate preference between viral and human thymidine kinase.

Thymidine kinase (TK, EC 2.7.1.21) is the key enzyme in the pyrimidine salvage pathway catalyzing the phosphorylation of thymidine (dT)[1] to thymidine monophosphate (dTMP) in the presence of $Mg^{2+}$ and ATP (*4*). $TK_{HSV1}$ accepts a broad range of substrates, in contrast to cellular TK (*5*−*8*). The antiviral compounds are selectively activated through phosphorylation by $TK_{HSV1}$ to finally act in their triphosphorylated form as DNA polymerase inhibitor as well as DNA chain terminators (*5*, *6*, *9*, *10*). The broad clinical use of aciclovir has led to the emergence of drug-resistance, mainly linked to $TK_{HSV1}$ mutations (*11*).

The rising resistance poses increasing problems for immunocompromised patients (*12*). Several new prodrugs have been developed and documented in large clinical trials (*12*−*16*). All of them are aciclovir analogues with improved oral bioavailability, however, showing cross-resistance because they are chemically similar and bind similarly to $TK_{HSV1}$ (*17*−*19*). Further searches for resistance-repellent

[†] This work was supported by the Graduiertenkolleg "Strukturbildung in makromolekularen Systemen" at the Albert-Ludwigs-Universität Freiburg.

[‡] The coordinate data-sets have been deposited in the Protein Data Bank at Brookhaven, MA, as 1E2K and 1E2L.

* To whom correspondence should be addressed. Phone: ++41-1-635 6036; Fax: ++41-1-635-6884; E-mail: scapozza@pharma.ethz.ch.

[§] Swiss Federal Institute of Technology (ETH).

[||] These authors contributed equally to this work.

[⊥] Albert-Ludwigs-Universität.

[#] Present address: Department of Biological Chemistry and Molecular Pharmacology, Harvard Medical School, 250 Longwood Ave., Boston, MA 02115.

[▽] Present address: Department of Biochemistry & Biophysics, Texas A&M University, College Station, TX 77843.

[▼] National Cancer Institute, National Institutes of Health.

[1] Abbreviations: MCT, 2′-*exo*-methanocarba-thymidine, (North)-methanocarba-thymidine; dT, (2′-deoxy)thymidine; dTMP, (2′-deoxy)-thymidine monophosphate; hTK1, human cytosolic thymidine kinase isoenzyme 1; $TK_{HSV1}$, thymidine kinase from Herpes simplex virus type 1.

10.1021/bi000668q CCC: $19.00 
Published on Web 07/14/2000

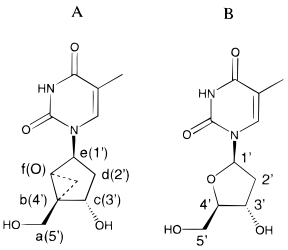


FIGURE 1: Covalent structure of MCT (A) and dT (B). The numbering for MCT is according to the nucleoside nomenclature used for dT in (*23*), and the cyclopropane ring of the conformationally restricted bicyclo[3.1.0]hexane is shown using a dashed line.

drugs led to $TK_{HSV1}$-circumventing monophosphate analogues (*20*−*22*) such as adefovir and cidofovir, which are active against a broad spectrum of DNA viruses, including *Herpes simplex* virus (types 1 and 2) (*20*).

A novel series of drugs is composed of conformationally rigid compounds that differ as little as possible from the natural substrate (*23*−*26*). Several of them were synthesized (*23*, *27*−*29*) and tested for antiviral activity against HSV1, HSV2, human cytomegalovirus, and Epstein−Barr virus. Very potent activity against HSV1 and HSV2 was discovered for MCT [2′-*exo*-methanocarba-thymidine; the 2′ position is defined according to the nucleoside numbering of (*23*) and corresponds to d(2′) of Figure 1].

The enzyme−prodrug gene therapy using $TK_{HSV1}$ as suicide gene (*30*−*32*) resembles the classical antiviral therapy. In this approach, the $TK_{HSV1}$ gene is introduced into tumor cells by retroviral or adenoviral vectors. Thus, dividing cells that express $TK_{HSV1}$ are capable of converting nontoxic nucleoside analogues such as ganciclovir into their nucleoside triphosphates which inhibit cellular polymerases leading to cell death and consequently tumor ablation (*33*−*37*). Clinical trials with ganciclovir were hampered by unfavorable side-effects such as immunosuppression caused by the large dosages required. Designing $TK_{HSV1}$ mutants with improved specificity toward the prodrug is therefore a useful endeavor (*38*−*40*). Here we present a $TK_{HSV1}$ mutant designed for gene therapy, characterize its properties in complex with the prodrug MCT, and relate these data to the interaction of MCT with the wild-type enzyme.

## MATERIALS AND METHODS

*Materials*. [*methyl*-1′,2′-$^3$H]Thymidine (3 TBq/mmol) was obtained from Amersham. Nucleotides and AmpliTaq Gold polymerase were from Perkin-Elmer. Restriction endonucleases, T4 DNA ligase, and thrombin were from Promega. Reagents for enzyme assays were obtained from Sigma. Strain DH5α (Clontech) was used for the cloning steps of the mutant. Strain BL21 (Pharmacia) served as expression host. The plasmids pGEX-2T, pGEX-6P-2, and the PreScission protease were purchased from Pharmacia. The plasmid pBR322-TK containing the TK gene of HSV1 strain F was a gift from S. McKnight. The plasmid pGEM-hTK containing the gene of the human cytosolic TK1 from lymphoctes was a gift from R. Hofbauer. Linbro plates and cover slides were purchased from Hampton Research; the sitting drop bridges were from DROP. All other reagents including the components of the protease-specific cleavage buffer were purchased from Fluka.

*Protein Engineering*. The active site mutant Y101F was constructed using the polymerase chain reaction based on the three-primer method (*41, 42*). The mutagenic primer (Y101F: 5′-GCG AAC ATC *TTC* ACC ACA CAA C-3′) and the M13 universal primer (5′-GCT ATG ACC ATG TTA CG-3′) were from Microsynth (Balgach, CH). The DNA fragment containing the desired mutation was cloned into the expression vector pGEX-2T-TK by digestion with the restriction enzymes *Bam*HI and *Kpn*I. This resulted in pGEX-2T-TK(Y101F) encoding for the thrombin-cleavable fusion protein of glutathione-*S*-transferase with $TK_{HSV1}$(Y101F).

*Sequence Verification.* Competent *E. coli* DH5α cells were transfected with pGEX-2T-TK(Y101F). After DNA isolation from several clones, the entire gene of the mutant was sequenced using the dye terminator method (ABI PRISM 310) to exclude additional mutations or frameshifts.

*Protein Expression and Purification.* Wild-type $TK_{HSV1}$ was produced using the expression vector pGEX-6P-2-TK coding for a PreScission protease-cleavable glutathione-*S*-transferase fusion protein. Mutant $TK_{HSV1}$(Y101F) and human cytosolic TK1 were expressed using vector pGEX-2T-TK(Y101F) and pGEX-6P-2-hTK1, respectively. All three proteins were expressed in *E. coli* strain BL21 as glutathione-*S*-transferase fusion proteins using a modified version of the previously published protocol (*43*). For purification, we only used glutathione affinity chromatography. The crude extract derived from 1 L of bacterial culture was applied 5 times to the glutathione Sepharose column and then washed in three steps with buffer A (1 M NaCl in 50 mM Tris, pH 7.5, 10% glycerol, 1 mM DTT, 0.1% Triton X-100), buffer B (250 mM $KH_2PO_4$/$Na_2HPO_4$, 150 mM NaCl, 0.1% Triton X-100, pH 7.0), and buffer C (250 mM $KH_2PO_4$/$Na_2HPO_4$, 150 mM NaCl, 0.1% Triton X-100, 10 mM MgATP, pH 7.4). Buffer C removed the 70 kDa protein DnaK (*44*). The column was then equilibrated with the protease-specific cleavage buffer. Thrombin cleavage of $TK_{HSV1}$(Y101F) was carried out at room temperature during 2 h. For wild-type $TK_{HSV1}$ and hTK1, the cleavage with PreScission protease was performed overnight at 4 °C. The eluted proteins were monitored by SDS−PAGE using both Coomassie and silver staining and showed a purity higher than 98% measured by densitometry.

*Assessment of Phosphorylation Pattern*. Phosphorylation of dT and MCT was monitored by high-performance liquid chromatography using a previously published protocol based on reverse-phase ion-pair chromatography (*45*). Blank reactions without enzyme or without substrate were run concurrently to account for background ATP hydrolysis. The detection limit for phosphorylated substrates lies at 20 nmol (*45*). The reactions were performed during 30 min with 70 μg/mL $TK_{HSV1}$, $TK_{HSV1}$(Y101F), or hTK1 in the presence of 2 mM substrate, 5 mM ATP, and 5 mM of $Mg^{2+}$.

*Kinetics*. Kinetic studies measuring the conversion of $^3$H-labeled dT to dTMP in the presence of various concentrations of MCT were performed using the DEAE-cellulose method (*46, 47*). Reactions were carried out in 30 μL of 50 mM Tris-HCl, pH 7.2, 5 mM ATP, 5 mM $MgCl_2$, 1.5 mg/mL BSA. The appropriate amount of enzyme and concentrations of [$^3$H]thymidine were chosen for Michaelis−Menten conditions for initial velocity measurements. The concentration of the compound was varied according to their affinity toward thymidine kinase. The $K_i$ values of MCT were determined by a nonlinear fit of the raw data to the

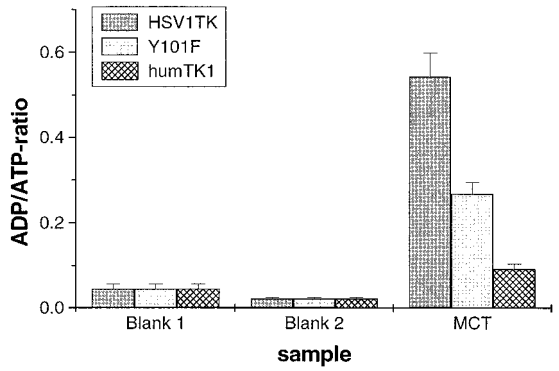


FIGURE 2: Histogram of the ADP/ATP ratios measured in MCT phosphorylation with wild-type $TK_{HSV1}$, $TK_{HSV1}$(Y101F), and hTK1. The control experiments show the ATP hydrolysis without MCT (Blank 1) and without enzyme (Blank 2). The standard deviations are given as vertical bars. The experiments were performed in triplicate using 2 mM MCT. All reaction assays started with 5 mM ATP and 5 mM $Mg^{2+}$ and no ADP.

equation: $V = V_{max}[dT]/\{K_M(1 + [compound]/K_i) + [dT]\}$ for competitive inhibition (*48*) using the Systat 5.02 software (Systat Inc., Evanston, IL). The $K_M$ and $V_{max}$ values of dT have been determined by nonlinear fit of the raw data to the Michaelis−Menten equation using the Microcal Origin software. $k_{cat}$ values for dT were determined by dividing $V_{max}$ by the enzyme concentration. The calculated values were based on at least three independent experiments.

*Crystallization*. Both $TK_{HSV1}$ and $TK_{HSV1}$(Y10F) were concentrated to 25 mg/mL by ultrafiltration using Centricon 30 concentrators. $TK_{HSV1}$(Y101F) was cocrystallized with MCT at a final concentration of 1 mM. Crystallization screenings were carried out at 23 °C by mixing equal volumes of reservoir and protein solution to obtain sitting and hanging drops. The best crystals grew from 0.9−1.2 M $Li_2SO_4$, 1 mM DTT, and 0.1 M HEPES at pH 8.0. They reached maximal sizes of 500 × 400 × 100 $\mu m^3$. Complex $TK_{HSV1}$/MCT was produced by soaking crystals in 5 mM MCT for 30 min.

Complex $TK_{HSV1}$/MCT diffracted X-rays isotropically to beyond 1.7 Å resolution at a synchrotron source whereas $TK_{HSV1}$(Y101F)/MCT diffracted to 2.4 Å using X-rays from a rotating anode (Table 2). Both crystals belong to space group $C222_1$ and contained two subunits of $M_r$ 40 972 and 37 169 for $TK_{HSV1}$/MCT and $TK_{HSV1}$(Y101F)/MCT, respectively.

*Data Collection*. Crystals were transferred into crystallization buffer supplemented by 30% (v/v) glycerol and then flash-frozen to 100 K. Data were collected using a MAR300 image plate with a 0.3 mm diameter collimator and Cu Kα radiation from a rotating anode generator (Rigaku, model RU2HC) at 45 kV and 120 mA. Further data collection was performed at 100 K on EMBL beamline BW7B at DESY (Hamburg) with a MAR345 image plate. All diffraction data were processed using the programs MOSFLM, SCALA, and TRUNCATE (*49*).

*Refinement*. As starting model we used the polypeptide of complex $TK_{HSV1}$/dTMP/ADP (*17*). After positioning the model as a rigid-body, atom positions and temperature factors were refined, alternating with modeling sessions. All refinement and electron density map calculations were performed with program REFMAC (*49*) using the same protocol for both structures $TK_{HSV1}$/MCT and $TK_{HSV1}$(Y101F)/MCT. The initial steps included noncrystallographic restraints within the dimer. Later on, individual *B*-factors were applied, and water molecules were added automatically using program ARPP (*49*). Sulfate ions and substrate molecules were introduced manually. In the last refinement cycles, the noncrystallographic restraints were completely removed. The *B*-values assigned for individual atoms of $TK_{HSV1}$/MCT ranged form 15 to 70 (maximum 120) and from 20 to 67 (maximum 92) for the protein and solvent, respectively. The *B*-values for $TK_{HSV1}$(Y101F)/MCT are comparable to those of $TK_{HSV1}$/MCT. The maximal *B*-values have been assigned to amino acids in the proximity of the protein parts that are highly mobile and have not been inserted in to the model (see below). Modeling was done using the program O (*50*). The programs MOLSCRIPT (*51*) and RASTER3D (*52*) were used for figure production.

## RESULTS

*Protein Engineering*. $TK_{HSV1}$(Y101F) was constructed by oligonucleotide-directed polymerase chain reaction mutagenesis. The mutated gene was entirely sequenced, confirming that only the designed mutation was present. Wild-type $TK_{HSV1}$, mutant $TK_{HSV1}$(Y101F), and human TK1 were expressed in *E. coli* as glutathione-*S*-transferase fusion proteins and purified to homogeneity and high purity by a one-step affinity chromatography as described. The thrombin and PreScission protease cleavage products were directly used for crystallization and enzyme kinetics.

*MCT Phosphorylation Pattern*. The phosphorylation was determined by monitoring the decrease of ATP, the increase of ADP, the formation of MCT-monophosphate, and the disappearance of MCT. The ADP/ATP ratios summarized in Figure 2 show ADP formation for wild-type and mutant $TK_{HSV1}$ that is clearly above the background ATP hydrolysis. The ADP/ATP ratio for human cytosolic thymidine kinase with MCT was less significant, compared to the negative controls. The ADP/ATP ratios demonstrate that MCT is phosphorylated quite efficiently by wild-type $TK_{HSV1}$ and by mutant Y101F, but at a much smaller rate by the human cytosolic thymidine kinase.

*Kinetics*. Competition studies were performed with wild-type $TK_{HSV1}$, $TK_{HSV1}$(Y101F), and hTK1 using $^3$H-labeled thymidine and MCT as competitive "inhibitor". Initial velocities ($V_i$) were determined by monitoring the increase of $^3$H-labeled dTMP at various MCT concentrations. The results are summarized in Table 1. $TK_{HSV1}$ showed a $K_i$ value of 11.4 $\mu$M for MCT. For mutant $TK_{HSV1}$(Y101F) and for hTK1, the $K_i$ values were 51.5 and 1600 $\mu$M, respectively. These data indicate the same trend as the phosphorylation pattern (Figure 2). Furthermore, $TK_{HSV1}$(Y101F) showed a 12-fold increase in $K_M$ for dT ($K_M$ = 2.5 $\mu$M) compared to the wild-type enzyme [$K_M$(dT) = 0.2 $\mu$M].

Using the phosphorylation data of Figure 2 and equating the $K_i$ with $K_M$ for MCT, we derived the specificity (*53*) of these three enzymes taking into account that, within a cell, endogenous dT would compete with MCT for the active site. By this calculation, a decrease of the value corresponds to an increase of specificity for MCT (Table 1). It turned out that wild-type $TK_{HSV1}$ has a 3 times higher value than the mutant $TK_{HSV1}$(Y101F), indicating that the mutant is 3 times more specific for MCT than the wild-type enzyme when

Table 1: Enzyme Kinetics for dT and MCT

| | dT[a] | | | MCT | | |
|---|---|---|---|---|---|---|
| enzyme | $K_M$ ($\mu$M) | $k_{cat}$ ($s^{-1}$) | rate[b] (%) | $K_i$ ($\mu$M) | rate[c] (%) | specificity[d] |
| $TK_{HSV1}$ | 0.20 ± 0.05 | 0.35 ± 0.02 | 100 | 11.4 ± 1.6 | 100 | 57 |
| $TK_{HSV1}$(Y101F) | 2.5 ± 0.5 | 0.19 ± 0.05 | 54 | 51.5 ± 5.1 | 53 | 20 |
| hTK1 | 0.49 ± 0.08 | 0.71 ± 0.18 | 203 | 1570 ± 200[e] | 9 | 72000 |

[a] Data at [MCT] = 0. [b] Relative phosphorylation rate calculated from the determined $k_{cat}$. [c] Relative phosphorylation rates derived from the data of Figure 2 accounting for background ATP hydrolysis. [d] The specificity is defined as the quotient of the catalytic efficiency ($k_{cat}/K_M$) of dT over MCT with $k_{cat}$ expressed as the relative phosphorylation rate: [rate(dT)/$K_M$(dT)]/[rate(MCT)/$K_i$(MCT)]. For MCT, we equated $K_i$ to $K_M$ (*60*). [e] The data could only be fitted by Lineweaver−Burk.

Table 2: Data Collection and Refinement Statistics

| data set[a] | $TK_{HSV1}$/MCT | $TK_{HSV1}$(Y101F)/MCT |
|---|---|---|
| diffraction data | | |
| X-ray source | BW7B | Cu $K_\alpha$ |
| unit cell (Å) | $a = 114.0$ | $a = 114.0$ |
| | $b = 117.7$ | $b = 118.3$ |
| | $c = 108.2$ | $c = 108.6$ |
| resolution range (Å) | 20−1.7 | 20−2.4 |
| completeness (%) | 99 | 97 |
| multiplicity | 4.1 | 3.4 |
| unique reflections | 79549 | 27908 |
| $R_{sym}$[b] (last shell) (%) | 5.0 (58) | 8.4 (50) |
| $I/\sigma$ (last shell) | 10.1 (2.1) | 11.3 (3.1) |
| refinement and final model | | |
| $R$-factor ($R_{free}$) (%) | 20.9 (25.2) | 21.1 (27.9) |
| average $B$-factor ($Å^2$) | 33 | 38 |
| protein atoms | 4761 | 4686 |
| substrate atoms | 36 | 36 |
| water molecules | 364 | 151 |
| sulfate ions | 2 | 2 |

[a] Crystals were of space group $C222_1$. All data were collected at 100 K. [b] $R_{sym} = \Sigma_h\Sigma_i I_{hi} - \langle I_h\rangle/\Sigma_h\Sigma_i I_{hi}$ where $h$ stands for the unique reflections and $i$ counts through symmetry-related reflections.

competition for the active site is considered. The value for the specificity of hTK1 is more than 1000 times higher than wild-type $TK_{HSV1}$, which means that the human enzyme prefers dT against MCT much more stringently. Together, we suggest that the mutant could constitute an improvement for gene therapy.

*High-Resolution Structure of $TK_{HSV1}$/MCT*. Complex $TK_{HSV1}$/MCT crystallized in space group $C222_1$ with two subunits per crystallographic asymmetric unit. The structure has been refined to 1.7 Å resolution (Table 2). This is the highest resolution yet reported for $TK_{HSV1}$. The final $R$-factor was 20.9% ($R_{free}$ = 25.2%). Only residue Arg163 is in a disallowed region of the Ramachandran diagram in both subunits (*54*). This is known from other analyses and may be due to a participation of this residue in catalysis (*17*−*19*, *55*, *56*). Some protein parts had no electron density, most likely they are highly mobile. These are residues 1−45, 72−75, 149−152, 266−278, and 375−376 of subunit A, and residues 1−45, 148−150, 221−224, 268−273, and 375−376 of subunit B. Each subunit contained a MCT molecule that was clearly defined in its electron density. The overall $\alpha\beta$ fold of the enzyme is conserved compared to the previously solved $TK_{HSV1}$ structures (*17*, *18*).

Like dT the thymine ring of MCT is stacked between Met128 and Tyr172 (Figure 3) and fixed by a hydrogen bond network. The strong hydrogen bonds of N3 and O4α with the Gln125 side chain resemble those of complex $TK_{HSV1}$/dT (*17*, *18*). The two water-mediated hydrogen bonds from O2α of the thymine ring to Arg176 are also present. The hydroxyl group of Tyr172 forms hydrogen bonds to His58 and Arg163, which in turn makes a water-mediated hydrogen bond to the sulfate ion bound in the *P*-loop at the same position as the $\beta$-phosphate of ADP in the $TK_{HSV1}$/dT/ADP structure solved using crystals grown under different crystallization conditions (*17*).

The well-defined electron density reveals clearly the ring pucker conformation of the sugar-mimicking moiety of MCT. The pucker is less pronounced in subunit A ($\nu_{max}$ = 9°), corresponding to a deviation of 0.35 Å of the carbon atom d(2′) (Figure 1) compared to the enzyme-free structure (*57*, *58*). In subunit B, the pseudosugar is slightly more puckered with a $\nu_{max}$ of 13° and a deviation of 0.25 Å. These deviations are clearly above the coordinate error. The values of *P* are, respectively, 21.9° and 351.9°, clearly in the northern hemisphere of the pseudorotational cycle (*59*). Therefore, the cyclopentane ring of the bicyclo[3.1.0]hexane system resembles a "planar pseudoboat". The pucker of MCT differs from the natural substrate dT in complex with $TK_{HSV1}$ (Figure 4) (*17*, *18*). The c(3′)-OH group of the pseudosugar moiety (Figure 1), the analogue of the 3′-OH of the deoxyribose of dT, is positioned at a distance of 3.7 Å to Glu225 and 4.1 Å to Tyr101-OH (4.0 Å in subunit B), indicating that, unlike dT, no direct hydrogen bonds are present for this moiety of the molecule. The direct hydrogen bond between Glu225 and the 3′-OH of dT reported in the structures of $TK_{HSV1}$ in complex with dT (*17*, *18*) is partially compensated by a water-mediated hydrogen bond between the c(3′)-OH group of MCT and Glu225 (Figures 1, 3, and 4). These structural observations are in agreement with the kinetic data and explain the difference in affinity between dT and MCT (Table 1). The a(5′)-OH group of MCT is fixed by a direct hydrogen bond to Glu83 (3.1 Å in subunit A; 3.5 Å in subunit B) and two water-mediated hydrogen bonds with Glu83 and Arg163 (Figure 3).

*Structure of $TK_{HSV1}$(Y101F)/MCT*. The complex of MCT with the active site mutant Y101F was refined to 2.4 Å resolution, yielding an $R$-factor of 21.1% ($R_{free}$ = 27.9%) (Table 2). The ($F_o - F_c$) map confirmed the successful mutation Y101F. Neither the polypeptide chain nor MCT showed significant changes in position or mobility compared to the wild-type complex.

The superposition of $TK_{HSV1}$/MCT with $TK_{HSV1}$(Y101F)/MCT shows a 1.0 Å shift of His58 away from residue 101. The two hydrogen bonds involving the hydroxyl group of Tyr101 and residue His58, on the one hand, and the water molecule ligated with the O2α of MCT, on the other hand, are lost by mutating this residue to Phe (Figure 3). This agrees with the kinetic data (Table 1). In the structures of $TK_{HSV1}$/dT/ADP and $TK_{HSV1}$/dT (*17*, *18*), the 3′-OH group

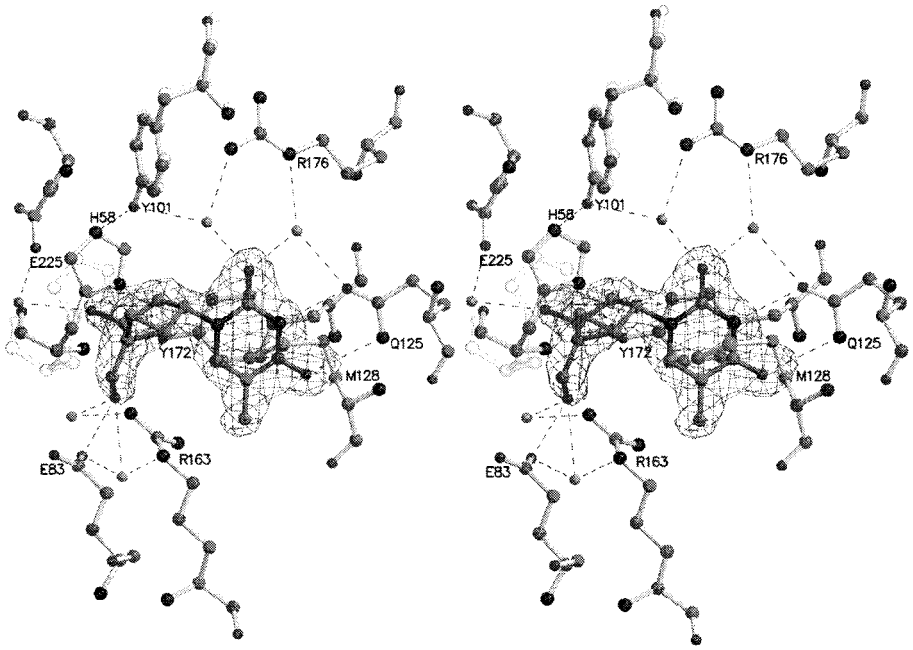


FIGURE 3: Stereoview of MCT binding at $TK_{HSV1}$ and $TK_{HSV1}$(Y101F). Only the mutation-dependent shift of 1.0 Å of residue His58 away from the mutated residue 101 is shown for $TK_{HSV1}$(Y101F). All other residues of the mutant which take the same conformation as in the wild-type complex were omitted for clarity reason. The conformation of the compound is well-defined by the $(2F_o - F_c)$ electron density contoured at a contour level of 1.3 $\sigma$. $TK_{HSV1}$ and $TK_{HSV1}$(Y101F) are shown in dark and light gray, respectively. Hydrogen bonds are depicted as dashed lines, water molecules as gray balls.

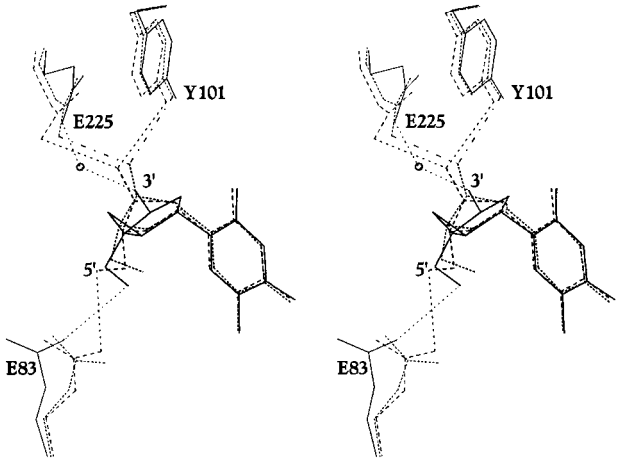


FIGURE 4: Superposition of $TK_{HSV1}$/MCT and $TK_{HSV1}$/dT structures. The structure of $TK_{HSV1}$/MCT is shown as continuous lines, $TK_{HSV1}$/dT in the same space group $C222_1$ *(18)* is shown in narrow dotted lines, and the structure of $TK_{HSV1}$/dT/ADP in space group $I4_1$ *(17)* is depicted in wide dotted lines. Hydrogen bonds are depicted as dashed lines, the water molecule as a black circle. For the sake of clarity, the dT hydrogen bonds are only depicted for the 3′-OH and 5′-OH groups. The hydrogen pattern for the thymine moiety is the same for all complexes and corresponds to that reported in Figure 3.

of the sugar moiety forms a hydrogen bond to Tyr101; therefore, its mutation to Phe weakens the binding of dT. The complex with MCT is not affected by this mutation as this substrate does not form any hydrogen bond to the hydroxyl group of Tyr101 (Figure 4).

## DISCUSSION

In solution, the sugar ring of nucleosides and nucleotides equilibrates between two extreme forms, a 2′-*exo*/3′-*endo* conformation and a 2′-*endo*/3′-*exo* conformation (*59*). On binding into the active site, one particular conformation is fixed, causing an unfavorable entropy contribution. The bound conformation can be mimicked in solution by introduction of a conformationally restricted sugar moiety reducing the unfavorable entropy contribution. For this purpose, a variety of nucleobases with a bicyclo[3.1.0]-hexanecarbocyclic analogue were synthesized in the past (*23*, *27*−*29*), and their antiviral activity was tested against several types of DNA viruses, such as HSV1 and HSV2, human CMV, and Epstein−Barr virus. Among them, MCT showed a high and reproducible antiviral activity against HSV1 and HSV2 as measured by plaque reduction assays. Its potency surpassed that of aciclovir (*23*).

The interaction of MCT with $TK_{HSV1}$, the prodrug activating enzyme in classical antiviral therapy, was studied. The phosphorylation of MCT could be demonstrated, indicating that the antiviral activity is probably linked to the thymidine salvage pathway in analogy to aciclovir. Knowing the enzyme structure, we constructed the active site mutant Y101F with increased acceptance of MCT and concomitant decreased dT utilization. $TK_{HSV1}$(Y101F) was indeed able to phosphorylate MCT to an extent comparable to the wild-type enzyme while dT utilization was clearly decreased. Furthermore, $TK_{HSV1}$(Y101F) showed the role of the fixed sugar ring pucker during the enzyme reaction.

Kinetic studies with MCT were performed with wild-type $TK_{HSV1}$, $TK_{HSV1}$(Y101F), and hTK1. On one hand, the binding behavior of the three enzymes toward dT was characterized by the Michaelis constant $K_M$. On the other hand, the affinity of MCT was determined by means of an inhibition study ($K_i$) because radiolabeled MCT was not readily available. We equated the measured $K_i$ value with $K_M$ because it has been previously demonstrated that both $K_M$ and $K_i$ of substrates of $TK_{HSV1}$, such as dT and aciclovir, correspond to the dissociation constant (*60*). The difference

in $K_i$ for MCT between the viral and human enzymes indicates the selectivity of the compound for the viral protein and explains the low toxicity detected for in vitro cell systems (*23*).

The binding mode of the MCT to $TK_{HSV1}$ is analogous to that of dT. The difference in binding affinity between the two substrates is clearly related to the loss of direct hydrogen bonds between the sugar moiety of the substrate to Tyr101 and Glu225. The binding affinity of the mutant for MCT is only 4.5 times lower than that of the wild-type, which contrasts with the corresponding dT affinities showing a 12-fold difference.

Because of the specificity shift, $TK_{HSV1}$(Y101F) can be considered a tailor-made enzyme for MCT. Together they constitute a new lead for enzyme−prodrug gene therapy approaches for which the bystander effect, that is reduced by pyrimidine-based prodrugs (*61*), is not necessary for increasing the therapeutic efficacy. An example of such an approach is the TK-controlled graft-versus-host disease in allogeneic bone marrow transplantation (*32*).

The crystal structures confirmed the kinetic measurements, showing that the conformationally restricted sugar ring pucker stabilizes MCT in a substrate-like position without using additional hydrogen bonds. The loss of two hydrogen bonds compared to the natural substrate thymidine is partly compensated by the entropy gain on ribose ring fixation. This entropic effect also explains the low susceptibility of MCT toward changes at position 101 that strongly influence binding of the natural substrate, thymidine. Although the pseudosugar ring conformation is known from ab initio calculations and from the crystal structure to be almost a perfect 2′-*exo* envelope ($P = 343.3°$ with a maximum puckering amplitude of 30°) (*57*, *58*), conformational changes on binding to the enzyme have to be expected. The 1.7 Å resolution structure of the complex now showed the ring pucker is smaller than that of the unligated compound.

Concluding, the biochemical characterization and the structures of MCT in complex with $TK_{HSV1}$ and mutant $TK_{HSV1}$(Y101F) demonstrate the advantage of a fixed ribose ring. MCT is certainly a novel lead in the search for resistance-repellent drugs in antiviral therapy. Moreover, in the context of improving enzyme−prodrug-mediated gene therapy, the results of this study show that it is possible to create tailor-made enzymes for conformationally rigidified prodrugs exploiting entropy.

## ACKNOWLEDGMENT

We thank the team of the EMBL-outstation Hamburg for help with synchrotron data collection.

## REFERENCES

1. Roizman, B. (1996) *Proc. Natl. Acad. Sci. U.S.A. 93*, 11307−11312.
2. Roizman, B., and Sears, A. (1996) *Herpes simplex viruses and their replication*, 3rd ed., Lippincott-Raven Publishers, Philadelphia.
3. Umene, K., and Sakaoka, H. (1999) *Arch. Virol. 144*, 637−656.
4. Okazaki, R., and Kornberg, A. (1964) *J. Biol. Chem. 239*, 275−284.
5. Elion, G. B., Furman, P. A., Fyfe, J. A., de Miranda, P., Beauchamp, L., and Schaeffer, H. J. (1977) *Proc. Natl. Acad. Sci. U.S.A. 74*, 5716−5720.
6. Fyfe, J. A., Keller, P. M., Furman, P. A., Miller, R. L., and Elion, G. B. (1978) *J. Biol. Chem. 253*, 8721−8727.
7. Keller, P. M., Fyfe, J. A., Beauchamp, L., Lubbers, C. M., Furman, P. A., Schaeffer, H. J., and Elion, G. B. (1981) *Biochem. Pharmacol. 30*, 3071−3077.
8. Reardon, J. E., and Spector, T. (1989) *J. Biol. Chem. 264*, 7405−7411.
9. McGuirt, P. V., and Furman, P. A. (1982) *Am. J. Med. 73*, 67−71.
10. Cheng, Y. C., Grill, S. P., Dutschman, G. E., Nakayama, K., and Bastow, K. F. (1983) *J. Biol. Chem. 258*, 12460−12464.
11. Coen, D. M. (1991) *Antiviral Res. 15*, 287−300.
12. Wutzler, P. (1997) *Intervirology 40*, 343−356.
13. Vere Hodge, R. A., Sutton, D., Boyd, M. R., Harnden, M. R., and Jarvest, R. L. (1989) *Antimicrob. Agents Chemother. 33*, 1765−1773.
14. Fife, K. H., Barbarash, R. A., Rudolph, T., Degregorio, B., and Roth, R. (1997) *Sex. Transm. Dis. 24*, 481−486.
15. Grant, D. M., Mauskopf, J. A., Bell, L., and Austin, R. (1997) *Pharmacotherapy 17*, 333−341.
16. Ida, M., Kageyama, S., Sato, H., Kamiyama, T., Yamamura, J., Kurokawa, M., Morohashi, M., and Shiraki, K. (1999) *Antiviral Res. 40*, 155−166.
17. Wild, K., Bohner, T., Folkers, G., and Schulz, G. E. (1997) *Protein Sci. 6*, 2097−2106.
18. Champness, J. N., Bennett, M. S., Wien, F., Visse, R., Summers, W. C., Herdewijn, P., de Clerq, E., Ostrowski, T., Jarvest, R. L., and Sanderson, M. R. (1998) *Proteins: Struct., Funct., Genet. 32*, 350−361.
19. Bennett, M. S., Wien, F., Champness, J. N., Batuwangala, T., Rutherford, T., Summers, W. C., Sun, H., Wright, G., and Sanderson, M. R. (1999) *FEBS Lett. 443*, 121−125.
20. De Clercq, E., Holy, A., Rosenberg, I., Sakuma, T., Balzarini, J., and Maudgal, P. C. (1986) *Nature 323*, 464−467.
21. Holy, A., Dvorakovy, H., Declercq, E. D. A., and Balzarini, J. M. R. (1994) patent WO9403467.
22. Holy, A., and Masojidikova, M. (1995) *Coll. Czech. Chem. Commun. 60*, 1196.
23. Marquez, V. E., Siddiqui, M. A., Ezzitouni, A., Russ, P., Wang, J., Wagner, R. W., and Matteucci, M. D. (1996) *J. Med. Chem. 39*, 3739−3747.
24. Scapozza, L., and Folkers, G. (1998) *Int. Antiviral News 6*, 210−213.
25. Ono, N., Iwayama, S., Suzuki, K., Sekiyama, T., Nakazawa, H., Tsuji, T., Okunishi, M., Daikoku, T., and Nishiyama, Y. (1998) *Antimicrob. Agents Chemother. 42*, 2095−2102.
26. Sekiyama, T., Hatsuya, S., Tanaka, Y., Uchiyama, M., Ono, N., Iwayama, S., Oikawa, M., Suzuki, K., Okunishi, M., and Tsuji, T. (1998) *J. Med. Chem. 41*, 1284−1298.
27. Rodriguez, J. B., Marquez, V. E., Nicklaus, M. C., Mitsuya, H., and Barchi, J. J., Jr. (1994) *J. Med. Chem. 37*, 3389−3399.
28. Ezzitouni, A., Barchi, J. J. J., and Marquez, V. E. (1995) *J. Chem. Soc., Chem. Commun.*, 1345−1346.
29. Siddiqui, M. A., Ford, H. J., George, C., and Marquez, V. E. (1996) *Nucleosides Nucleotides 15*, 235−250.
30. Culver, K. W., Ram, Z., Wallbridge, S., Ishii, H., Oldfield, E. H., and Blaese, R. M. (1992) *Science 256*, 1550−1552.
31. Moolten, F. L. (1994) *Cancer Gene Ther. 1*, 279−287.
32. Bonini, C., Ferrari, G., Verzeletti, S., Servida, P., Zappone, E., Ruggieri, L., Ponzoni, M., Rossini, S., Mavilio, F., Traversari, C., and Bordignon, C. (1997) *Science 276*, 1719−1724.
33. Panis, Y., and Houssin, D. (1995) *Presse Med. 24*, 1681−1683.
34. Klatzmann, D. (1996) *Hum. Gene Ther. 7*, 255−267.
35. Sturtz, F. G., Waddell, K., Shulok, J., Chen, X., Snodgrass, H. R., and Platika, D. (1997) *Stereotact. Funct. Neurosurg. 68*, 252−257.
36. Nagy, H., Panis, Y., Fabre, M., Perrin, H., Klatzmann, D., and Houssin, D. (1998) *Surgery 123*, 19−24.
37. Tiberghien, P. (1998) *Curr. Opin. Hematol. 5*, 478−482.
38. Black, M. E., Newcomb, T. G., Wilson, H. M., and Loeb, L. A. (1996) *Proc. Natl. Acad. Sci. U.S.A. 93*, 3525−3529.

39. Encell, L. P., Landis, D. M., and Loeb, L. A. (1999) *Nat. Biotechnol. 17*, 143−147.
40. Kokoris, M., Sabo, P., Adman, E., and Black, M. (1999) *Gene Ther. 6*, 1415−1426.
41. Steinberg, R. A., and Gorman, K. B. (1994) *Anal. Biochem. 219*, 155−157.
42. Barettino, D., Feigenbutz, M., Valcarcel, R., and Stunnenberg, H. G. (1994) *Nucleic Acids Res. 22*, 541−542.
43. Fetzer, J., Michael, M., Bohner, T., Hofbauer, R., and Folkers, G. (1994) *Protein Express. Purif. 5*, 432−441.
44. Silva, N. L., Haworth, R. S., Singh, D., and Fliegel, L. (1995) *Biochemistry 34*, 10412−10420.
45. Pilger, B., Perozzo, R., Alber, F., Wurth, C., Folkers, G., and Scapozza, L. (1999) *J. Biol. Chem. 274*, 31967−31973.
46. Furlong, N. B. (1963) *Anal. Biochem. 5*, 515−522.
47. Gerber, S., and Folkers, G. (1996) *Biochem. Biophys. Res. Commun. 225*, 263−267.
48. Segel, I. R. (1993) *Enzyme kinetics*, Wiley, pp 102 ff, Wiley, New York.
49. CCP4. (1994) *Acta Crystallogr. D 50*, 760−763.
50. Jones, T. A., Zou, J. Y., Cowan, S. W., and Kjeldgaard. (1991) *Acta Crystallogr. A 47*, 110−119.
51. Kraulis, P. J. (1991) *J. Appl. Crystallogr. 24*, 946−950.
52. Merritt, E. A., and Bacon, D. J. (1997) *Methods Enzymol. 277*, 505−524.
53. Christians, F. C., Scapozza, L., Crameri, A., Folkers, G., and Stemmer, W. P. (1999) *Nat. Biotechnol. 17*, 259−264.
54. Laskowski, R. A., MacArthur, M. W., Moss, D. S., and Thornton, J. M. (1993) *J. Appl. Crystallogr. 26*, 283−291.
55. Wild, K., Bohner, T., Aubry, A., Folkers, G., and Schulz, G. E. (1995) *FEBS Lett. 368*, 289−292.
56. Brown, D. G., Visse, R., Sandhu, G., Davies, A., Rizkallah, P. J., Melitz, C., Summers, W. C., and Sanderson, M. R. (1995) *Nat. Struct. Biol. 2*, 876−881.
57. Marquez, V. E., Ezzitouni, A., Siddiqui, M. A., Russ, P., Ikeda, H., and George, C. (1997) *Nucleosides Nucleotides 16*, 1431−1434.
58. Altmann, K.-H., Kesselring, R., Francotte, E., and Rihs, G. (1994) *Tetrahedron Lett. 35*, 2331−2334.
59. Saenger, W. (1984) *Principles of nucleic acid structure*, pp 51−104, Springer-Verlag, New York.
60. Kussmann-Gerber, S., Wurth, C., Scapozza, L., Pilger, B. D., Pliska, V., and Folkers, G. (1999) *Nucleosides Nucleotides 18*, 311−330.
61. Degreve, B., De Clercq, E., and Balzarini, J. (1999) *Gene Ther. 6*, 162−170.

BI000668Q